Communication

A Peptoid Square Helix via Synergistic Control of Backbone Dihedral Angles.

Benjamin Craig Gorske, Emily M Mumford, Charles G Gerrity, and Imelda Ko

J. Am. Chem. Soc., **Just Accepted Manuscript** • Publication Date (Web): 24 May 2017

A Peptoid Square Helix via Synergistic Control of Backbone Dihedral Angles.

Benjamin C. Gorske,* Emily M. Mumford, Charles G. Gerrity, and Imelda Ko.

*Department of Chemistry, Bowdoin College, 6600 College Station, Brunswick, Maine 04011-8466.
Email: bgorske@bowdoin.edu

Supporting Information Placeholder

ABSTRACT: The continued expansion of the fields of macromolecular chemistry and nanoscience has motivated the development of new secondary structures that can serve as architectural elements of innovative materials, molecular machines, biological probes, and even commercial medicines. Synthetic foldamers are particularly attractive systems for developing such elements because they are specifically designed to facilitate synthetic manipulation and functional diversity. However, relatively few predictive design principles exist that permit both rational and modular control of foldamer secondary structure, while maintaining the capacity for facile diversification of displayed functionality. We demonstrate here that the synergistic application of two such principles in the design of peptoid foldamers yields a new and unique secondary structure that we term an "η-helix" due to its repeating turns, which are highly reminiscent of peptide β-turns. Solution-phase structures of η-helices were obtained by simulated annealing using nOe-derived distance restraints, and the NMR spectra of a series of designed η-helices were altogether consistent with the primary adoption of this structure. The structure is resilient to solvent and temperature changes, and accommodates diversification without requiring post-synthetic manipulation. The unique shape, broad structural stability, and synthetic accessibility of η-helices could facilitate their utilization in a wide range of applications.

Interest in developing foldameric, and particularly peptidomimetic, oligomers is on the rise as evidence of their remarkable utility and versatility in the development of new bioactive compounds, catalysts, materials, and even medicines continues to accrue.[1,2] Peptoids (*N*-alkylglycine oligomers) have proven to be especially adaptable platforms for such applications, as their conception was strongly motivated by considerations of synthetic facility and structural diversity.[3] The nearly equal energies of peptoid amide bond rotamers enable control of the ω-dihedral angle (Figure 1) via relatively weak intramolecular interactions,[4] which have been engineered to stabilize new secondary structures such as peptoid ribbons,[5] helices,[6] and Σ-strands.[7] The capacity to rationally program the ω-dihedral angle simply by sidechain choice and without additional synthetic manipulation distinguishes peptoids from most other foldamers and endows them with unique structural and functional capabilities. The peptoid ribbon secondary structure that arises from alternating incorporation of *cis*- and *trans*-amide-promoting 1-naphthylethyl and phenyl sidechains, respectively, aptly demonstrates the application of this design principle.[5] However, design strategies of comparable scope for per-residue control of the other peptoid backbone dihedral angles (ψ and ϕ) are much less developed. We recently reported one such strategy entailing the tandem incorporation of enantiomeric 1-naphthylethyl sidechains that can be used to rationally "switch" the backbone ϕ angle.[8] However, the "ω-strand" structures resulting from alternation of (*S*)- and (*R*)-1-naphthylethyl sidechains did not dominate the conformational manifold at oligomer lengths exceeding four residues.

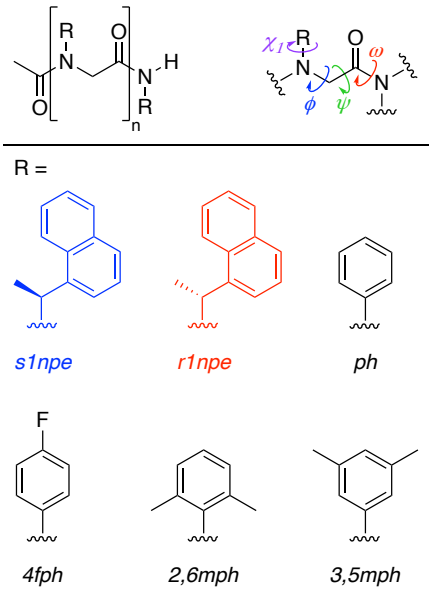

FIGURE 1. Structures of the peptoid oligomers and side chains examined in this study.

We now report that the synergistic application of the two strategies above — incorporation of both enantiomeric side chains and side chains that alternately promote *cis*- and *trans*-amides in the backbone — yields a new and unique peptoid secondary structure. We refer to this structure as an "η-helix" since it resembles a peptide π helix with longer facets. NMR spectroscopy revealed that these structures exhibit high conformational homogeneity, are highly insensitive to solvent perturbation, and tolerate phenyl sidechain diversity. We thus envision that η-helices will complement eminent peptoid secondary structures such as helices, ribbons, and Σ-strands in the construction of new materials, catalysts, and biologically active compounds.

We first examined trimer **1** representing the shortest possible unit that permits both alternation of the *cis*- and *trans*-promoting sidechains (1-naphthylethyl and various phenyl residues, respectively) and alternation of the 1-naphthylethyl sidechain stereoconfiguration (Figure 1, Table 1). Although other peptoid secondary structures can require up to 12 residues to achieve conformational homogeneity due to reliance on cooperative folding,[7] we observed a dominant conformation by NMR spectroscopy in CD_3OD for trimer **1**, suggesting that the sidechains exert a high degree of local structural control, as observed in peptoid ribbons.[5] In contrast to the peptoid ω-strands that we recently reported,[8] elongation of the trimer up to octamer length (**2**–**5**) in accordance with the design principal above did not significantly impact conformational homogeneity.

Table 1. Peptoid oligomer structures.

compound	monomer sequence
1	*r1npe*-*ph*-*s1npe*
2	*3,5mph*-*r1npe*-*ph*-*s1npe*
3	*s1npe*-*3,5mph*-*r1npe*-*ph*-*s1npe*
4	*4fph*-*s1npe*-*3,5mph*-*r1npe*-*ph*-*s1npe*
5	*2,6mph*-*r1npe*-*4fph*- -*s1npe*-*3,5mph*-*r1npe*-*ph*-*s1npe*
6	*4fph*-*r1npe*-*3,5mph*-*s1npe*
7	*s1npe*-*4fph*-*r1npe*-*3,5mph*-*s1npe*
8	*2,6mph*-*r1npe*-*3,5mph*-*s1npe*
9	*r1npe*-*2,6mph*-*s1npe*
10	*2,6mph*-*r1npe*-*ph*-*s1npe*
11	*r1npe*-*3,5mph*-*s1npe*

The solution-phase structure of pentamer **3** in CD_3OD was obtained by simulated annealing using distance restraints derived from key inter-residue nOes (Figure 2). Notably, the incorporation of enantiomeric *1npe* residues provided sufficient dispersion to unambiguously assign each peak of interest without isotopic labeling. Consistent with previously reported solution- and solid-phase structures of peptoid helices and ribbons, the 1-naphthylethyl sidechains clearly enforced the adoption of the *cis*-rotamer (ω dihedral angle ≈ 0°) by the preceding residue, as evidenced by strong nOes between the *i* and *i*-1 methylene protons.[4d,5] In contrast, the achiral but *trans*-amide-promoting (ω dihedral angle ≈ 180°) *N*-aryl residues produced nOes between the methylene and sidechain protons within the residue, as observed in previous studies of *N*-aryl PPII-like helices and peptoid ribbons.[5,6c] Restraining the simulated annealing using these nOe-based ω-angle restraints, along with key nOes observed between the *1npe* methyl groups and sidechain protons of the *i*+1 and *i*+2 residues, yielded several compact structures that were inconsistent with the paucity of additional inter-residue nOes observed. Thus, absent distance restraints (ADRs) were used (in a manner consistent with that employed to determine the extended peptoid helix structure[6a]) to penalize structures that would give rise to strong but unobserved nOes to the *3,5mph* methyl groups.

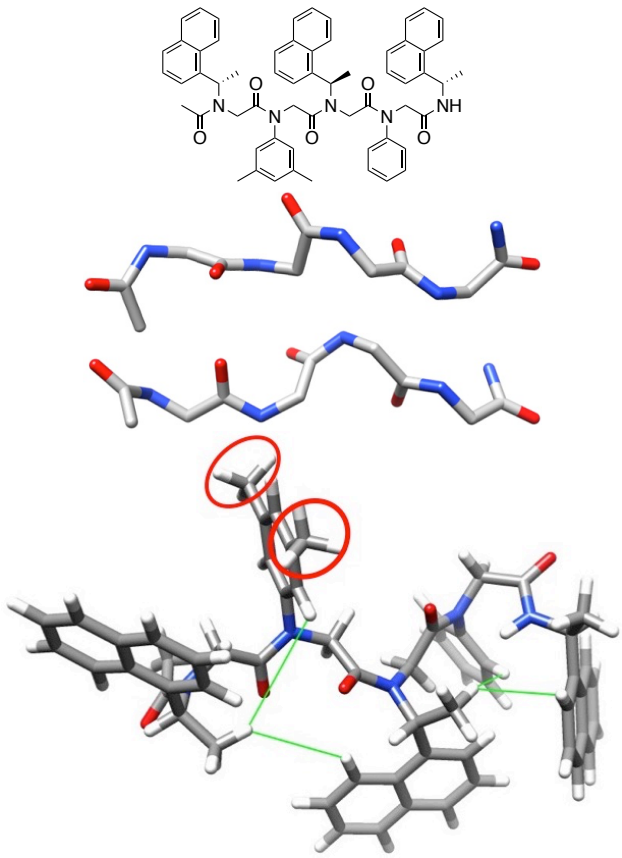

FIGURE 2. Top: Chemical structure of **3**. Middle: Views of the lowest energy structure obtained from nOe-

restrained simulated annealing of **3**. (Hydrogen atoms and sidechains removed for clarity.) Bottom: Lowest energy structure from simulated annealing with key nOes and ADRs in green and red, respectively.

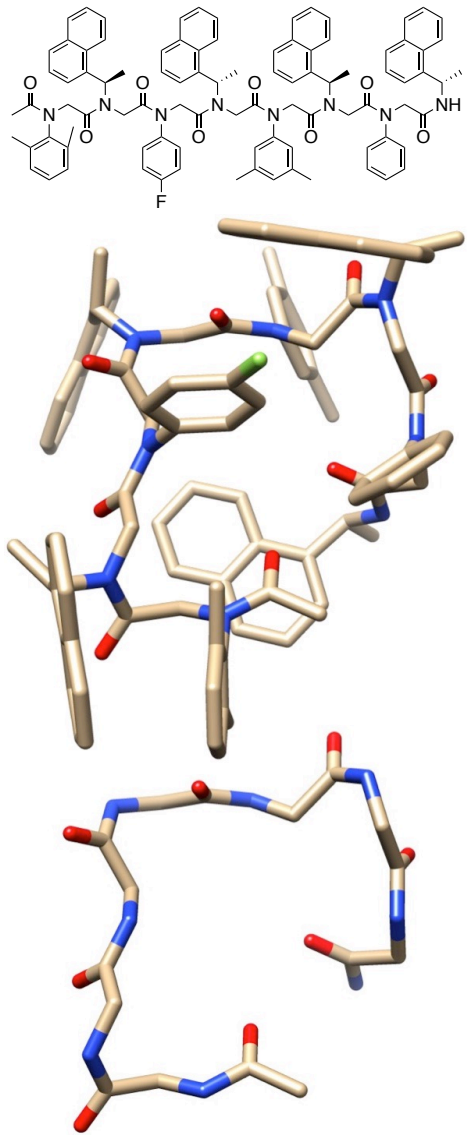

FIGURE 3. Chemical structure of **5**, and the lowest energy structure obtained from nOe-restrained simulated annealing of octamer **5** with (top) and without (bottom) sidechains. (Hydrogen atoms removed for clarity.)

The ensemble of the ten lowest energy structures exhibited a RMSD of 1.05 Å, and each of these structures was wholly consistent with the complete set of observed nOes (see Supporting Information). Aside from the *C*-terminal residue containing a unique secondary amide, the dihedral angles closely correspond to those of a peptoid ribbon, except that the signs of the ϕ angles alternate between positive and negative for *s1ne* and *r1ne*, respectively. Thus, the stereoconfiguration of the 1-naphthylethyl sidechain apparently dictates the ϕ dihedral angle, with the *S*- and *R*-enantiomers enforcing ϕ angles of approximately –60° and +60°, respectively; this particular relationship between primary and secondary peptoid structure is precedented within the context of peptoid ω-strands.[8] As is typical for peptoids, the ψ angles uniformly cluster near 180°. The minimal repeating unit containing both *S*- and *R*-sidechains is tetrameric and contains both central and terminal turns for which the η-helix is named. The NMR spectra of both longer peptoids (**4** and **5**) and peptoids containing differently substituted phenyl groups in various positions (**6**–**11**) are also universally consistent with the elucidated structures, regardless of solvent (see Supporting Information). The similar nOe patterns observed in CD_3OD, CD_3CN, and $CDCl_3$ for the principal conformations of compounds **1**–**11** suggest that steric interactions play the dominant role in their folding. Variable-temperature NMR spectroscopy of trimer **1** in CD_3CN revealed no spectral perturbation of consequence between -40 and 80 ºC, further supporting this hypothesis.

In order to further explore the structural space accessible using the titular design strategy, we also obtained a solution-phase structure for octamer **5** in CD_3CN (Figure 3) using nOe-restrained simulated annealing and assignments of the backbone methylene protons based on the NMR-derived structure of **3**. (Although **5** was also soluble in CD_3OD, insufficient dispersion was obtained for unambiguous assignment of the resonances.) In addition to the inter-residue nOes of the types observed for **3**, **5** also exhibited several nOes between the *C*- and *N*-termini, and between the termini and central residues, that collectively focused the simulated annealing outcomes to yield the compact solution-phase structure shown. The ensemble of lowest energy structures reveals consecutive pairs of 90° turns that completely reverse the direction of the backbone. As a result, the residues appended to the termini of internal turns (e.g. *4fph* and *ph*, *2,6mph* and *3,5mph*) are arrayed approximately parallel to each other, analogously to a peptide β-hairpin. (The *C*-terminal residue containing the secondary amide once again adopted an outlying conformation as observed in pentamer **3**.) This parallel orientation is enabled in part by the counterbalancing of the gentle backbone curvatures produced by the *s1ne* and *r1ne* residues, leading to a more flattened structure compared to peptoid ribbons comprised of only one of these enantiomeric residues.[5] The antiparallel alignment of the residues protruding from the turns distinguishes them from the more obtuse, corkscrew-like turns observed in peptoid ribbons. We attribute the unique, ≈90° angles in the η-helix backbone to steric interactions between these antiparallel residues that force slight deviations of the backbone

dihedral angles from their predicted optimal values. Thus, the backbone flexibility afforded by relying solely upon noncovalent interactions for folding appears to play a critical role in the formation of these helices. This flexibility is presumably also responsible for the planar displacement of the *C*- and *N*-termini, resulting in one terminus "tucking under" the other to provide a slight pitch to the nascent square helix. In conclusion, we have elucidated a new peptoid secondary structure realized by rational, synergistic control of both the ω and ϕ backbone dihedral angles using only noncovalent interactions. To our knowledge, this particular foldamer construction approach, which maximizes synthetic and structural flexibility by obviating covalent cyclization of backbone atoms, has not been reported previously. The insensitivity of the structure to variation of solvent and temperature indicates that steric interactions provide the primary impetus for folding. Such broad structural competence suggests that η-helices that are appropriately functionalized and solubilized using existing, well-developed strategies for peptoids[7,9] could serve as useful scaffolds in a variety of contexts. Inspired by peptide β-hairpins that have proven to be privileged catalyst scaffolds due to their capacity to aggregate functionality and engender bifunctional catalysis,[10] we are currently developing η-helix-derived β-hairpins as catalysts. Indeed, the internal turns of octamer **5** place the side chains of the antiparallel residues in close proximity, which could facilitate both mimicry of multifunctional enzyme active sites and cyclization. Furthermore, such hairpins could serve to nucleate strand-like structures as they do in peptides.[11] We thus envision grafting more linear peptoid structures such as ω- or Σ-strands,[7,8] and perhaps even PPI- and PPII-type helices,[6] to isolated η-helix turns to generate peptoid β-sheet mimics. The structure of octamer **5** suggests that such sheets could be stabilized by π-stacking of interdigitated aromatic groups rather than by interstrand hydrogen bonding, and we are thus actively investigating these possibilities in our laboratory. We also submit that η-helical peptidic structures can be accessed using suitably modified D- and L-amino acids; such residues might be used within the context of η-helix/peptide hybrid oligomers to control the ψ dihedral angles, potentially yielding complete modular control of the entire backbone.[12] Overall, this work demonstrates the generality of structural control achievable using enantiomeric sidechains in peptidomimetics, and further illustrates the versatility of peptoids as a foldameric system.

Supporting Information. The Supporting Information is available free of charge on the ACS Publications website.

ACKNOWLEDGMENT

We wish to thank Dr. Ronald Zuckermann for helpful and contributive discussions, and Prof. Amelia Fuller for CD spectroscopy. Acknowledgment is made to the Donors of the American Chemical Society Petroleum Research Fund for support of this research. Support for the LCMS instrumentation at Bowdoin College by the NSF (CHE-1126657) is gratefully acknowledged.

REFERENCES

(1) (a) Gellman, S. H. *Acc. Chem. Res.* **1998**, *31*, 173–180. (b) Hill, D. J.; Mio, M. J.; Prince, R. B.; Hughes, T. S.; Moore, J. S. *Chem. Rev.* **2001**, *101*, 3893–4012. (c) Martinek, T. A.; Fülöp, F. *Chem. Soc. Rev.* **2012**, *41*, 687–702.

(2) (a) Kritzer, J. A.; Lear, J. D.; Hodsdon, M. E.; Schepartz, A. *J. Am. Chem. Soc.* **2004**, *126*, 9468–9469. (b) Zuckermann, R. N.; Kodadek, T. *Curr. Opin. Mol. Ther.* **2009**, *11*, 299–307. (c) Maayan, G.; Ward, M. D.; Kirshenbaum, K. *Proc. Nat. Acad. Sci. U.S.A.* **2009**, *106*, 13679–13684. (d) Lee, M. M.; Pushechnikov, A.; Disney, M. D. *ACS Chem. Biol.* **2009**, *4*, 345–355. (e) Gan, Q.; Ferrand, Y.; Bao, C.; Kauffmann, B.; Grélard, A.; Jiang, H.; Huc, I. *Science* **2011**, *331*, 1172–1175. (f) Gopalakrishnan, R.; Frolov, A. I.; Knerr, L.; Drury, W. J., III; Valeur, E. *J. Med. Chem.* **2016**, *59*, 9599–9621.

(3) Zuckermann, R. N.; Kerr, J. M.; Kent, S. B. H.; Moos, W. H. *J. Am. Chem. Soc.* **1992**, *114* (26), 10646–10647.

(4) (a) Gorske, B. C.; Blackwell, H. E. *J. Am. Chem. Soc.* **2006**, *128*, 14378–14387. (b) Gorske, B. C.; Bastian, B. L.; Geske, G. D.; Blackwell, H. E. *J. Am. Chem. Soc.* **2007**, *129*, 8928–8929. (c) Gorske, B. C.; Stringer, J. R.; Bastian, B. L.; Fowler, S. A.; Blackwell, H. E. *J. Am. Chem. Soc.* **2009**, *131*, 16555–16567. (d) Stringer, J. R.; Crapster, J. A.; Guzei, I. A.; Blackwell, H. E. *J. Am. Chem. Soc.* **2011**, *133*, 15559–15567. (e) Caumes, C.; Roy, O.; Faure, S.; Taillefumier, C. *J. Am. Chem. Soc.* **2012**, *134*, 9553–9556.

(5) Crapster, J. A.; Guzei, I. A.; Blackwell, H. E. *Angew. Chem. Int. Ed. Engl.* **2013**, *52*, 5079–5084.

(6) (a) Armand, P.; Kirshenbaum, K.; Goldsmith, R. A.; Farr-Jones, S.; Barron, A. E.; Truong, K. T.; Dill, K. A.; Mierke, D. F.; Cohen, F. E.; Zuckermann, R. N.; Bradley, E. K. *Proc. Nat. Acad. Sci. U.S.A.* **1998**, *95*, 4309–4314. (b) Wu, C. W.; Kirshenbaum, K.; Sanborn, T. J.; Patch, J. A.; Huang, K.; Dill, K. A.; Zuckermann, R. N.; Barron, A. E. *J. Am. Chem. Soc.* **2003**, *125*, 13525–13530. (c) Shah, N. H.; Butterfoss, G. L.; Nguyen, K.; Yoo, B.; Bonneau, R.; Rabenstein, D. L.; Kirshenbaum, K. *J. Am. Chem. Soc.* **2008**, *130*, 16622–16632.

(7) (a) Mannige, R. V.; Haxton, T. K.; Proulx, C.; Robertson, E. J.; Battigelli, A.; Butterfoss, G. L.; Zuckermann, R. N.; Whitelam, S. *Nature* **2015**, *526*, 415–420.

(8) Gorske, B. C.; Mumford, E. M.; Conry, R. R. *Org. Lett.* **2016**, 18, 2780–2783.

(9) Fuller, A. A.; Yurash, B. A.; Schaumann, E. N.; Seidl, F. J. *Org. Lett.* **2013**, *15*, 5118–5121.

(10) Metrano, A. J.; Abascal, N. C.; Mercado, B. Q.; Paulson, E. K.; Hurtley, A. E.; Miller, S. J. *J. Am. Chem. Soc.* **2017**, *139*, 492–516.

(11) Fuller, A. A.; Du, D.; Liu, F.; Davoren, J. E.; Bhabha, G.; Kroon, G.; Case, D. A.; Dyson, H. J.; Powers, E. T.; Wipf, P.; Gruebele, M.; Kelly, J. W. *Proc. Natl. Acad. Sci. U.S.A.* **2009**, *106*, 11067–11072.

(12) (a) Siebler, C.; Erdmann, R. S.; Wennemers, H. *Angew. Chem. Int. Ed. Engl.* **2014**, *53*, 10340–10344. (b) DeRider, M. L.; Wilkens, S. J.; Waddell, M. J.; Bretscher, L. E.; Weinhold, F.; Raines, R. T.; Markley, J. L. *J. Am. Chem. Soc.* **2002**, *124*, 2497–2505.

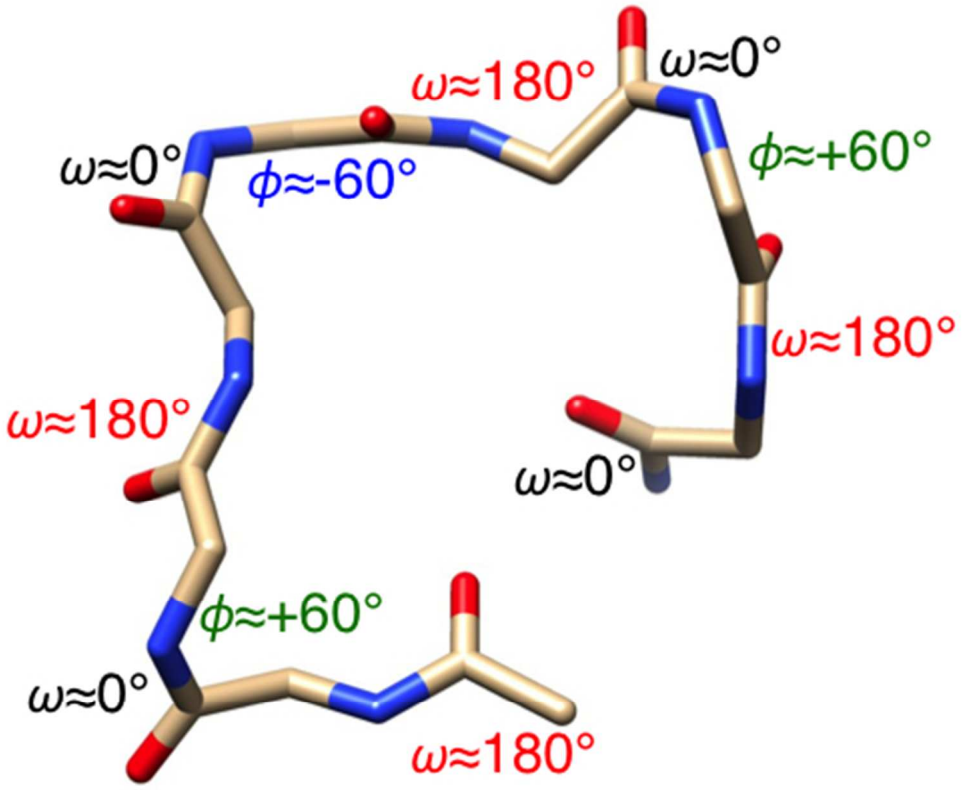

Revised TOC graphic

176x141mm (72 x 72 DPI)